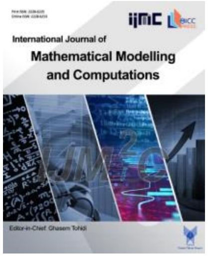

Int. J. Math. Model. Comput. 2026; 16(3): 190-206

International Journal of Mathematical Modelling & Computations (IJM^{2}C)

https://doi.org/10.57647/ijm2c.2026.1603.15

Research Article

Designing a Cat Robot with a Defective Leg Capable of Jumping Stairs

Mehrdad Naghs Nilchi, Mohammad Saadat*, Ali Soleimani, Meisam Vahabi, Mehdi Salehi

Department of Mechanical Engineering, Na.C., Islamic Azad University, Najafabad, Iran

***Corresponding author:** saadatpmc@gmail.com

Original Research:

Received:
7 October 2025

Revised:
9 December 2025

Accepted:
15 December 2025

Published Online:
24 December 2025

Published in issue:
30 September 2026

Abstract

Many scientists utilize the movement behavior of animals in nature to design and simulate robots. Jumping over obstacles is one of the most crucial and challenging tasks for four-legged robots. However, errors can occur when these robots attempt to jump on stairs. If one leg of the four-legged robot is defective, appropriate adjustments can be made to enable the robot to still jump on stairs. This paper focuses on simulating the jumping motion of a four-legged robot, which is considered one of the most challenging aspects of controlling such robots. Initially, a two-dimensional model of the four-legged robot is introduced, followed by the formulation of dynamic equations that govern the robot's jumping motion. This operation is subsequently simulated using Adams software, whereby the robot's jump is modeled through torsion springs in each leg. One of the most challenging scenarios discussed in this article involves the four-legged robot jumping on stairs with a defective leg. The robot's jump on the stairs is then optimized based on various parameters, and the best case scenario of the robot jumping on stairs with a defective leg is presented. This optimized case is illustrated in diagram form within the article.

Keywords: Four-legged; Robot jumping; Simulation; Dynamic; Fault-tolerant

Cite this article: Naghsh Nilchi M, Saadat M, Soleimani A, Vahabi M, Salehi M. Designing a cat robot with a defective leg capable of jumping stairs. Int. J. Math. Model. Comput. 2026; 16(3): 190-206. doi: https://doi.org/10.57647/ijm2c.2026.1603.15

1. Introduction

One-legged and multi-legged robots have received considerable attention in recent years. Robots with wheel legs [1], one leg [2], three legs [3], five legs [4], seven legs [5], or even more legs [6] are relatively uncommon but feasible. Walking robots offer numerous advantages over wheeled and tracked robots, although they are generally more complex. This complexity stems not only from the mechanical mechanisms employed but also from the electronic systems and sensing/control algorithms implemented.

Meanwhile, extensive research has been conducted on four-legged robots, which possess significant flexibility in their movements. These robots are capable of performing various tasks due to their unique schematics. In essence, legged robots excel in navigating complex environments compared to other mobile robots [7]. They are particularly well-suited for tasks involving rough, irregular, and unstructured terrains, such as planetary exploration [8], urban rescue [9], and disaster response [10]. The movement of robots in unstructured environments remains one of the most challenging topics in mobile robotics [11].

The autonomy and stability of robots rely heavily on their ability to maintain stability while traversing uneven terrains [12], as well as their energy efficiency [13-14]. NaghshNilchi et al. [15], investigated the jumping of a quadruped robot on a step. In this study, they performed a detailed simulation of the four-legged robot using Adams software. The four-legged robot in this study had 3 torsional joints. Quan et al. [16] optimized the jumping path of a four-legged robot, known as the cheetah, by examining its kinematic relationships and considering certain limitations. Xuan et al. [17], performed a kinematic assessment of a single leg and performed a full-body simulation in ADAMS software. The results showed that maintaining a balanced body position significantly improved ground adaptation and joint efficiency. Coelho et al. [18] reviewed research conducted on six-legged robots, classifying articles based on numerical simulations, robot implementation, or a combination of both, as well as the type of robot movement environment and sensors used. Their findings indicate that in recent years, all three types of research (including simulation, implementation, and combined approaches) have had an equal share in studies on robust mobile robots. Moreover, research has predominantly focused on irregular laboratory environments and flat lands, followed by regular laboratory environments like stairs and ramps. The least amount of research has been dedicated to robot movement in external environments such as deserts or forests. Given the aforementioned cases, it can be concluded that robot jumping represents one of the newest and most challenging fields of active research in this domain.

Researchers have dedicated specific efforts to designing robots capable of overcoming obstacles such as stairs. Through various designs and control systems, several robots have successfully demonstrated their stair-climbing abilities. Examples include two-legged robots such as Cassie [19] and ASIMO [20], MIT Cheetah [21], Pegasus [22], Jueying [23], and Scalf [24]. Moreover, robots such as THU-QUAD II [25], ALPHRED [26], and Qingzhui [27] have utilized six-legged configurations. Mertyüz et al [28], designed and simulated a four-legged wheeled robot that was capable of crossing obstacles. In this paper, they analyzed the motions of the proposed robot in wheeled and legged modes. Liu et al. [29] investigated a six-legged robot with a defective leg on a ramp. After designing and simulating the six-legged robot, they studied its balance when one of its legs was damaged. The analysis demonstrated that the six-legged robot was capable of continuing its path even with one lost leg, even on inclined surfaces. Additionally, Sarkar et al. [30] modeled and analyzed the walking of a fault-tolerant six-legged robot on an inclined plane. In their research, the designed six-legged robot performed steadily at low speeds. In this research, a six-legged robot was designed to demonstrate the ability to continue moving and maintain balance even after one leg is broken. Tatar [31], simulated the jump of a robot whose legs were W-shaped. In this research, he first designed the robot and obtained kinematic relationships, then simulated the robot in software. The simulated robot could overcome unevenness. Han et al [32], designed a quadruped robot that was able to cross obstacles. They presented a newly developed energy-efficient obstacle crossing control framework, using which the robot was able to jump over obstacles with low energy consumption.Li et al [33], designed a six-legged robot with the ability to climb stairs. In this research, they examined the stair climbing of the six-legged robot in various cases. After simulation in ADAMS software, the six-legged robot was able to climb the stairs and reach the upper terrace. Li et al [34], modeled a quadruped robot with load-carrying capabilities. They then simulated their model in Adams software. The modeled robot was able to climb stairs with a height of 0.175 meters while carrying a load.

The paper focuses on examining the general equations governing the four-legged robot and obtaining the Dynavit-Hartenberg matrix required for robot modeling in the Adams software. The simulation of the four-legged robot in the Adams software closely resembles reality, resulting in highly accurate results. Specifically, the robot jump in this paper is based on the real case of a cat jumping with a defective leg, aiming for a more realistic and precise analysis.

To further enhance the modeling of the four-legged robot with a defective leg, software optimization was employed to achieve the best possible state while minimizing energy consumption during the jumping process. The optimizations performed are illustrated in the form of diagrams presented in the paper.

In other words, the important point to note in this article is the design of a four-legged robot capable of jumping despite having a defective leg.

2. Kinematic Model

In this study, the jump of the four-legged robot is simulated taking inspiration from the jumping ability of felines in nature. Felines are known to store energy in their leg muscles, which is then released to perform a jump over obstacles. To mimic this behavior, torsion springs are used as the "muscles" in the legs of the robot. By applying force to these springs, energy is stored in the reserve spring, similar to the way energy is stored in the leg muscles of felines. When the spring is released, the stored energy is utilized to propel the robot forward and perform the jump. Figure 1 depicts the two-dimensional model of the simulated four-legged robot, which incorporates these torsion springs in its leg design. This allows for a realistic representation of the jumping behavior observed in felines, enabling the robot to successfully navigate and overcome obstacles.

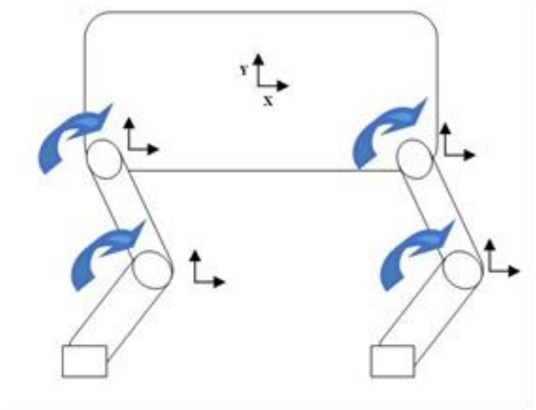

Figure 1. Two-dimensional model of cat robot

The hip and ankle joints in the robot are rotational joints, each equipped with a torsion spring that functions as a muscle. During the modeling process, the dimensions of the robot were carefully adjusted to match those of a pet with a limited carrying capacity. In this study, the dynamic model of the quadruped robot is formulated in two dimensions, focusing on the sagittal plane. The primary reason for adopting a 2D representation is that the dominant components of forward jumping (such as the center-of-mass trajectory, leg extension–compression behavior, spring energy storage, joint torques, and ground reaction forces) occur mainly within the sagittal plane. Numerous established studies on legged locomotion and jumping (e.g., Raibert's leg models [2], MIT Cheetah [21] jumping studies) also demonstrate that a 2D dynamic formulation is sufficient to accurately capture the essential mechanics of forward jumping motions. Using a 2D model prevents unnecessary computational complexity during optimization, as a full 3D model significantly increases the dimensionality of the problem (involving roll, yaw, lateral foot placement, and out-of-plane dynamics). Such complexity is not required for analyzing the main objective of this research, which is the effect of a defective leg on the jumping capability of the robot in a forward direction.

Table 1. Parameters of the 2D cat robot model

Parameter	Value
Dimensions of the robot body	(50cm×20cm×20cm)
knee length	12.5(cm)
Thigh length	12.5(cm)
Ankle dimensions	(7cm×6.5cm×4cm)
The total mass of the robot	36(Kg)

According to the parameters specified in Table 1 for the two-dimensional model of the four-legged robot, the total mass of the robot including its equipment and load is set at 36 kg.

Equation (1) shows configuration variables [14]:

$$Q = [x; y; q_{pitch}; q]. \tag{1}$$

Where x and y are COM position of the robot, q_{pitch} is the body pitch angle in the world frame, and q is the joint angle vector including hip and knee joint angles of front and back legs [35]. By using space vector algebra [36], the dynamic equations of the robot can be obtained in the form of an equation (2):

$$H(Q)\ddot{Q} + C(Q,\dot{Q})\dot{Q} + g(Q) + K(Q) = B\tau + B_{fric} + \tau_{fric}(Q) + \sum_{i} J_i^T(Q)F_i. \tag{2}$$

Where H is the mass matrix and the matrix C contains Coriolis and centrifugal terms. Also in equation (2), g is the gravity vector and J_i is the spatial Jacobian of the body containing the i^{th} foot expressed at the foot and in the world coordinate system; F_i is the spatial force at the i^{th} foot; matrices B and B_{fric} define how the actuator torques τ and the joint friction torques τ_{fric} enter the model. Also, K is stiffness matrix, with elements k_i representing the spring stiffness of each torsional joint (e.g., hip and knee joints). The term K(q) represents the elastic restoring torque provided by the torsional springs, which store potential energy during joint flexion according to $E = (1/2)\,k\,\theta^2$, where k is the spring stiffness and θ is the joint angle. This energy is released during joint extension, reducing the actuation torque required and enhancing energy efficiency during gait cycles. The inclusion of torsional springs distinguishes this model from traditional rigid-link designs, as it enables passive energy recovery, improves gait smoothness. In order to obtain the kinematics of the robot, first the movement of the body in space and the related generalized coordinates are defined. For this purpose, the Denavit-Hartenberg (DH) matrix is used. DH parameters from one leg shown in Figure 2.

Considering that each of the legs of the cat robot in this paper has three degrees of freedom, the parameters of the DH matrix will be extracted in the form of Table 2. It should be noted that the parameters in Table 2 were obtained based on the kinematics of the four-legged robot and the joints in each leg of the robot.

Table 2. DH Parameter

Link	$\alpha_{i,j}$	$a_{i,j}$	$d_{i,j}$	$\theta_{i,j}$
1	0	a_1	0	θ_1
2	0	a_2	0	θ_2

On the other hand, as shown in equation (3), the DH

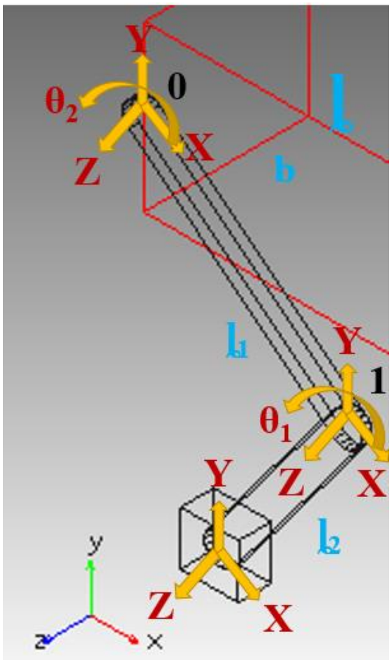

Figure 2. Reference variables for cat robot legs

matrix for the i^{th} joint is:

$$A_i^{i-1} = \begin{bmatrix} c\theta_i & -s\theta_i c\alpha_i & s\theta_i s\alpha_i & a_i c\theta_i \\ s\theta_i & c\theta_i c\alpha_i & -c\theta_i s\alpha_i & a_i s\theta_i \\ 0 & s\alpha_i & -c\theta_i s\alpha_i & d_i \\ 0 & 0 & 0 & 1 \end{bmatrix}. \quad (3)$$

As shown in equation (4), the matrix of each of the joints is:

$$A_1^0 = \begin{bmatrix} c_1 & -s_1 & 0 & a_1 c_1 \\ s_1 & c_1 & 0 & a_1 s_1 \\ 0 & 0 & 1 & 0 \\ 0 & 0 & 0 & 1 \end{bmatrix}, \quad A_2^1 = \begin{bmatrix} c_2 & -s_2 & 0 & a_2 c_2 \\ s_2 & c_2 & 0 & a_2 s_2 \\ 0 & 0 & 1 & 0 \\ 0 & 0 & 0 & 1 \end{bmatrix}. \quad (4)$$

Equation (5) shows the Jacobian matrix of the leg [29]:

$$J(q) = \begin{bmatrix} Z_0 \times (P - P_0) & Z_1 \times (P - P_1) & Z_2 \times (P - P_2) \\ Z_0 & Z_1 & Z_2 \end{bmatrix}. \quad (5)$$

In equation (5), z_0, z_1, z_2, are joint axes, p_0, p_1, p_2, are joint position vectors and p is the foot position vector. The submatrices of the Jacobian matrix are given in equation (6) and (7).

$$J(\theta_1) = \begin{bmatrix} -a_1 s_1 - a_2 s_{12} \\ a_1 c_1 + a_2 c_{12} \\ 0 \\ 0 \\ 0 \\ 1 \end{bmatrix}, \quad (6)$$

$$J(\theta_2) = \begin{bmatrix} -a_2 s_{12} \\ a_2 c_{12} \\ 0 \\ 0 \\ 0 \\ 1 \end{bmatrix}, \quad (7)$$

The dynamic model was validated through a combination of structural, numerical, and behavioral checks. First, the derived dynamic equations and DH matrices were cross-verified with standard rigid-body dynamics formulations (Featherstone [35], Sciavicco & Siciliano [36]) to ensure full theoretical consistency. Then, the model was implemented in ADAMS, and energy-conservation tests, analytical-to-numerical Jacobian comparisons, and motion-trend verification were performed. The simulated behavior of the healthy robot matched the patterns reported in established quadruped platforms (e.g., MIT Cheetah [21], NaghshNilchi et al. [15]). Furthermore, three independent optimization runs with different initial conditions converged to nearly identical optimal parameters, confirming the numerical stability of the model. Finally, the simulated behavior of the defective leg showed strong similarity to documented biomechanical patterns in cats with partial hind-leg dysfunction, supporting the biological plausibility of the proposed model.

The resulting equations allow for real-time computation of joint angles required for any desired foot position within the robot's reachable workspace. This capability is handy in adaptive jumping, navigating terrain, and avoiding obstacles.

3. Cat Robot Simulation

In this section, the simulation of the robot and its environment will be described. Due to the lengthy simulation process for this research, crucial explanations in the simulation are briefly mentioned in each section, and obvious details are omitted.

To simulate the behavior of the cat robot, the first step is to simulate a staircase. In order to broaden the scope of optimization, the staircase in this study is designed as a single point. This allows for flexibility in optimizing the dimensions of the stairs as needed. The coordinates of the stairs are listed in Table 3, and Figure 3 depicts the simulation of the stairs in the software.

In the next step, the cat robot is simulated in the Adams software based on the desired dimensions and size, as depicted in Figure 4. It is important to note that the distance between the robot and the first step is set to 60 cm.

After simulating all the components of the cat robot and the staircase, the necessary parameters for optimization need to be defined before introducing any disturbances

10.57647/ijm2c.2026.1603.15

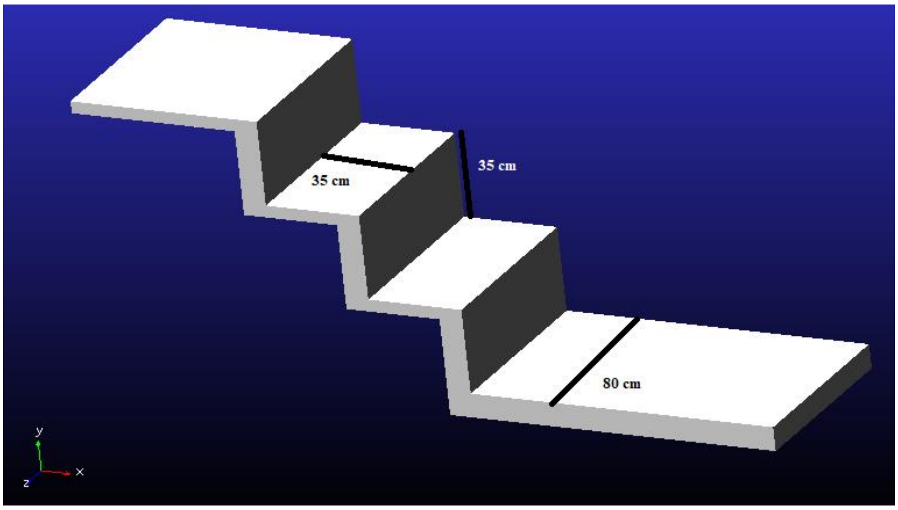

Figure 3. Designing stairs

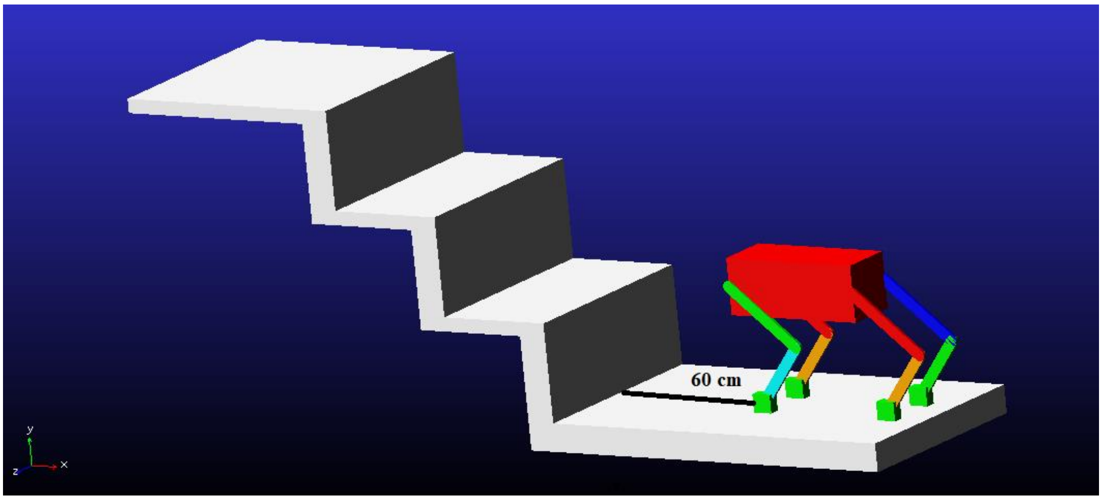

Figure 4. Simulated cat robot

to the robot's legs. Also, it should be noted that other aspects, such as the identification of "CONTACT FORCE" and similar details, were considered during the simulation.

After simulating the cat robot, the optimization and design assumptions and parameters are explained, followed by running the problem through the software.

4. Optimization

The main objective of this research is to optimize all the parameters that can significantly influence the jumping ability of the four-legged robot. Various "Design Variables" are employed in the software to facilitate this optimization process. Even the stiffness values of the torsion springs and the damper values in each joint are optimized. Additionally, considering the weight of the robot and other relevant parameters, approximate minimum and maximum values for these variables are determined to guide the software in determining the optimal values for spring stiffness and other parameters, aligning with the optimization goal.

ADAMS utilizes several optimization algorithms, and in this problem, the MSADC_SQP algorithm is employed**.** In other words, ADAMS provides several optimization algorithms (e.g., DOT_SQP, MMC, Genetic Algorithm, etc.). The MSADC_SQP (Modified Simulated Annealing Sequential Quadratic Programming) hybrid algorithm was deliberately selected for several reasons. The stair-jumping problem with a defective leg is highly nonlinear and contains multiple local minima due to discontinuous contact forces and unilateral constraints. Pure gradient-based methods (e.g., standard SQP) frequently converge to poor local optima when starting far from the global solution. MSADC_SQP combines the global search capability of Modified Simulated

Table 3. Stair design points

Point	X	Y	Z
1	0.1	0	0
2	-1.2	0	0
3	-1.2	0.35	0
4	-1.6	0.35	0
5	-1.6	7	0
6	-2	7	0
7	-2	1.05	0
8	-2.4	1.05	0
9	-2.8	1.05	0
10	-2.8	1	0
11	-2.1	1	0
12	-2.1	0.65	0
13	-1.7	0.65	0
14	-1.7	0.3	0
15	-1.3	0.3	0
16	-1.3	-0.1	0
17	0.1	-0.1	0
18	0.1	0	0

Annealing (to escape local minima) with the fast local convergence of SQP, which is particularly effective for legged robot trajectory optimization with contact discontinuities. In the design and simulation process of quadruped robots, optimization plays a crucial role in improving the robot's performance and efficiency. ADAMS software is one of the advanced tools in the field of motion simulation and dynamic analysis, using optimization algorithms to find the best values for various parameters. This process is especially important in jumping simulation, as it is necessary to accurately adjust parameters such as forces, torques, and joint angles to achieve optimal performance. Using optimization in ADAMS allows for the automatic identification of optimal values for different robot parameters. For instance, this method helps to find the best settings for forces acting on the robot’s joints, jump velocity, and angle. This process leads to more accurate analysis of the robot's behavior and the interactions between its components, improving the robot’s jumping performance. One of the significant advantages of using optimization in ADAMS is the reduction in the time and cost associated with trial-and-error during the design phase. Instead of conducting multiple experiments to test the robot's performance under different conditions, optimization in ADAMS enables us to quickly find optimal values and simulate the robot's behavior under various scenarios. This method enhance the accuracy of simulation results and reduces potential errors in the robot's design. Moreover, optimization in ADAMS uses sophisticated algorithms that simultaneously analyze all parameters, allowing for the identification of optimal values even in complex and nonlinear conditions. Specifically, during the jumping process, these algorithms can model the robot’s joint behavior in response to external forces, including gravity, ground impact, and various resistances, thereby providing optimal parameters for achieving the best jumping performance. Finally, the use of optimization in ADAMS not only improves the robot's performance in simulation but also ensures more accurate real-world implementation. With this method, we can be confident that the robot will achieve optimized jumps in reality, and its performance in the real world will align with the simulation results.To optimize the parameters, certain assumptions were made and briefly mentioned. In the optimization, the following constraints are applied:

$$\begin{aligned} q &\le q_{s\_k} \le \bar{q}, \\ \dot{q} &\le \dot{q}_{s\_k} \le \bar{\dot{q}}, \\ \ddot{q} &\le \ddot{q}_{s_k} \le \bar{\ddot{q}}. \end{aligned} \tag{8}$$

Where q and $\bar{q}$ are the upper and lower boundary matrices for the joint variables; $\dot{q}$ and $\bar{\dot{q}}$ are the upper and lower boundary matrices for the velocities;$\ddot{q}$and$\bar{\ddot{q}}$are the upper and lower boundary matrices for the accelerations, respectively. In this optimization, according to the designed robot model, the rotation joint angle in the robot's legs is limited between -30 degrees and +30 degrees. The linear spring can be compress maximum *7* cm. With regard to the capacity of the motor and gearbox, it is important to limit the output torques of the robot’s joints. Therefore, the following torque constraints are imposed:

$$\tau \le \tau_{s_K} \le \bar{\tau}. \tag{9}$$

Where, τ and $\bar{\tau}$ are the upper and lower boundaries of the torques. The initial posture of the robot is defined by:

$$\begin{aligned} q_{s\_i} &= q_{s_i,d}, \\ \dot{q}_{s\_i} &= \dot{q}_{s\_i,d}, \\ \ddot{q}_{s\_i} &= \ddot{q}_{s\_i,d}, \qquad \text{i=0…N.} \end{aligned} \tag{10}$$

Where$q_{s_i,d}$, $\dot{q}_{s\_i,d}$ and $\ddot{q}_{s\_i,d}$ are given joint variable, velocity, and acceleration vectors at time step 0 and N (the launch moment), respectively. Additionally, the effect of gravity is assumed to act opposite to the Y-axis with a value of 9.8 (m/s^2).

The optimization problem was formulated as a single-objective minimization of the total mechanical energy consumed by the four active actuators during one jumping cycle. The objective function is explicitly defined as:

10.57647/ijm2c.2026.1603.15

$$J = \int_0^T (|\tau_1(t).\omega_1(t)| + |\tau_2(t).\omega_2(t)| + |\tau_3(t).\omega_3(t)| + |\tau_4(t).\omega_4(t)|)dt. \quad (11)$$

Where:
- $\tau_i(t)$ and $\omega_i(t)$ are instantaneous torque and angular velocity of joint i (i = 1…4 correspond to left-hip, left-knee, right-hip, right-knee),
- The right hind knee and hip (defective leg) contribute $\tau = 0$,
- $T \approx 0.92$ s is the cycle duration obtained after optimization,
- Absolute value is used to account for both positive and negative (small) regenerative braking phases.

It is worth noting, no additional penalty or weighting terms are included; pure mechanical input energy of the actuators is minimized.

One of the primary objectives of this research is to optimize the energy consumption of a four-legged robot with a defective leg during stair jumping. The ideal scenario is for the robot, despite losing one leg, to execute the jump with the least amount of energy consumption and continue moving up the stairs consecutively. To achieve this, as depicted in Figure 5, the distance between the legs of the cat robot and the stairs should be minimized. These locations are defined at the beginning of each step in the Adams software.

According to Figure 5, there are 5 hip joints and 4 knee joints in the simulated cat robot. Table 4 presents the minimum and maximum limits of the "Design Variables" for all parameters that are utilized for optimization purposes.

Table 4. Design Variables for optimization

Design Variable	Min	Max
Stiffness	100	200
Damper	1	2
Torq	900	1500
Torq 2	1200	1800
Torq e1	2000	3000
Torq hb	0	1000
Torq hb2	500	2000
Torq h3	100	300
Torq 4F	1000	2300
Torq 4b	2000	3500
Torq 5f	900	2500
Torq 5b	1000	3000
Torq 6f	1000	3000
Torq 6b	2000	3000

It should be noted that the upper and lower limits in Table 4 are obtained based on trial and error, and all the units in Adams software are MKS. It should be noted that the entire optimization process is carried out from the "Design Exploration" module in the top toolbar of the software. In our study, the upper and lower bounds assigned to the optimization parameters (including joint torques and spring stiffness values) were selected based on a combination of mechanical design limits, dynamic feasibility, and iterative trial-and-error refinement within the ADAMS simulation environment.

To justify these ranges, we compared our parameter limits with values reported in well-established quadruped robot platforms in the literature. For instance, in the MIT Cheetah-3 [21], (one of the most prominent high-performance quadruped robots—the maximum joint torque capability is reported to be approximately 250 N·m.

In comparison, our robot model has a total mass of 36 kg, but unlike the platforms above, it performs stair-jumping maneuvers under asymmetric loading conditions due to a defective leg. This condition substantially increases the dynamic load on the healthy legs, particularly during take-off and landing phases. Consequently, higher torque bounds are mechanically expected for ensuring realistic and stable simulation behavior. Therefore, the torque bounds selected in Table 4 should not be interpreted as exact motor specifications, but rather as conservative limits that ensure physically plausible motion, prevent numerical divergence in ADAMS, and allow the optimizer to account for the increased loads caused by the missing support of one leg. Accordingly, the parameter ranges used in our optimization procedure are fully aligned with established practices in the literature, while appropriately adapted to the more demanding and asymmetric jumping scenario analyzed in this work.

Using the values specified in the aforementioned table, each value is assigned to the corresponding joint at the appropriate time and location. In Table 4, "Tork e1" represents the applied torque needed for the cat robot to maintain balance. "Tork hb" and "Tork h" denote the auxiliary torque applied to the joints of the cat robot and the rear joints of the robot during jumping, respectively. "Tork 4b," "Tork 5b," and "Tork 6b" signify the torque applied to the rear joints of the robot at different times. Similarly, "Tork 4f," "Tork 5f," and "Tork 6f" refer to the torque applied to the front joints of the cat robot at different times.

The main objective of optimizing and obtaining the best parameter values is to ensure the robot maintains balance while jumping and to minimize joint opening. Achieving this balance is crucial for the walking process.

One of the complex and crucial aspects addressed in this paper is the equations for the jumping of a robot with a defective leg. These equations encompass the magnitude

10.57647/ijm2c.2026.1603.15

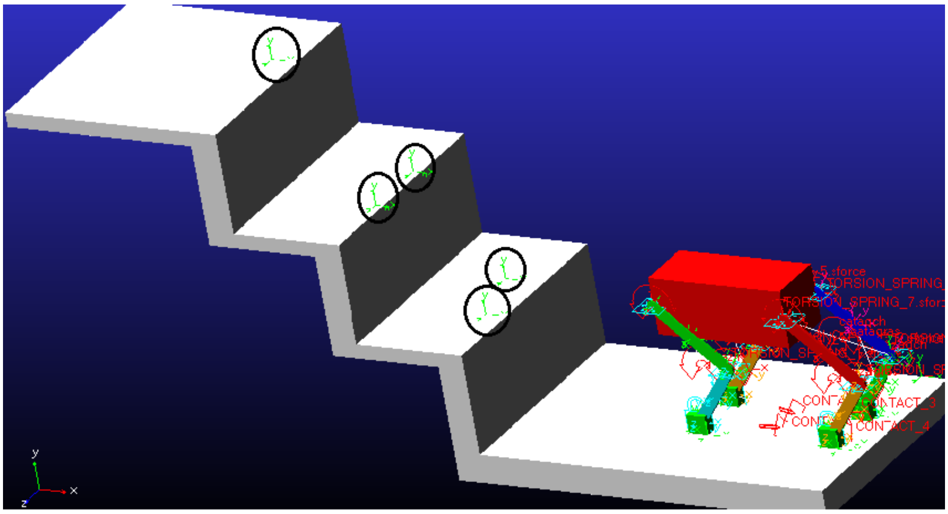

Figure 5. Defined points to optimize energy consumption

Figure 6. Movement behaviour of a cat with a defective leg

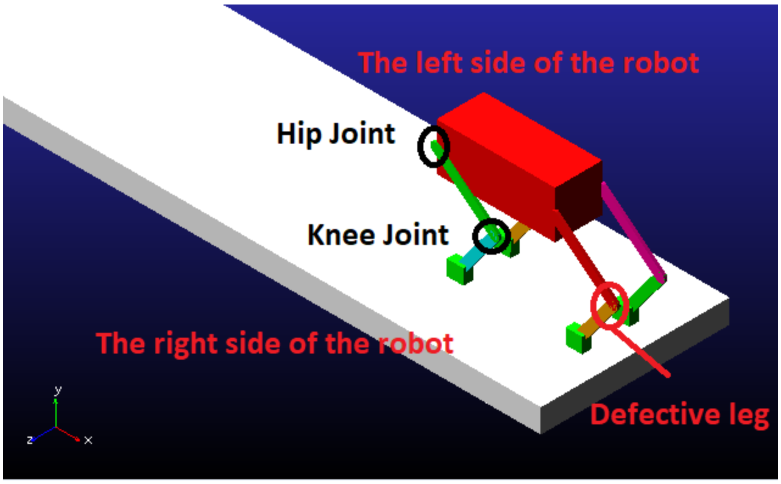

Figure 7. Simulated cat robot with a defective leg

10.57647/ijm2c.2026.1603.15

of force for jumping, the timing and extent of joint opening and closing during landing on each step, the joint angles for take-off and landing on the step with a defective leg, the energy input to the rear legs, auxiliary torque applied to the joints due to the presence of a defective leg, and other relevant factors.

Addressing these challenges was a key aspect of formulating the equations presented in this paper.

Through careful observation of cats with a broken leg, it is noticed that they employ their broken leg as a support while walking and jumping. Specifically, they use the broken leg primarily for maintaining balance and exert very minimal or no force on the defective leg. Figure 6 illustrates an example of a cat with a broken leg.

As seen in Figure 6, the cat's malformed foot is used as a support to maintain balance and assist other joints during stepping. The defective leg in this study is modeled to reflect a biologically realistic partial injury, such as partial joint failure or stiffness loss, rather than complete amputation. This is common in real cats, where hind leg injuries often involve limited range of motion (ROM), reduced joint stiffness, or partial torque loss without total loss of function. For instance, cats with cruciate ligament tears or degenerative joint disease exhibit stiffness, reduced ROM, and lower torque in the affected joint, yet they can still perform jumps and stair climbing by adapting their gait. On the other hand, the defective foot can still touch the ground or stair edge passively (contact stiffness and damping unchanged), matching real three-legged cat locomotion where the injured leg occasionally brushes the ground without providing significant propulsion. Also, the cat's defective leg is usually in the air while walking and makes less contact with the ground. Utilizing the same movement behavior, jump times, and other factors, the necessary equations for the different joints of the cat robot have been provided in the Adams software. Additionally, in order to simulate the cat robot with a defective leg, one of the robot's joints, as shown in Figure 7, is considered defective in the Adams software. The simulations account for several forces acting on the robot, including gravitational force, elastic forces from the legs, and impact forces during landing. By accurately simulating these interactions in ADAMS, a comprehensive analysis of the robot's performance under different jumping conditions is enabled.

5. Dynamic Equations of the Cat Robot Joints for Jumping Simulation

5.1. Defective Leg

In this section, the dynamic equations for the various joints of the quadruped robot are presented to model its jumping behavior in the ADAMS software. These equations are crucial for simulating the movement and interaction of the robot's legs, ensuring a realistic representation of the forces acting on the joints during the jump.

The model includes the following joints:

- Equation for the right front hip joint of the robot:

$$\begin{aligned} & step(time,2.5,0,3.5,torq) \\ & +step(time,3.6,0,3.601,-torq) \\ & +step(time,3.7,0,3.8,2*torq2) \\ & +step(time,5.2,0,6,torq4j) \\ & +step(time,6.1,0,6.101,-torq4j) \\ & +step(time,6,0,6.5,-2*torq2) \\ & +step(time,8.2,0,9,torq5j) \\ & +step(time,9.1,0,9.101,-torq5j) \\ & +step(time,9.2,0,9.5,torq) \\ & +step(time,11,0,12,-1*torq) \\ & +step(time,13.5,0,14,.catproject.torq6j) \\ & +step(time,14.1,0,14.101,-.catproject.torq6j). \end{aligned} \tag{13}$$

- Equation for the left front hip joint of the robot:

$$\begin{aligned} & step(time,2.5,0,3.5,torq) \\ & +step(time,3.4,0,3.601,-torq) \\ & +step(time,3.7,0,3.8,2*torq2) \\ & +step(time,5.2,0,6,torq4j) \\ & +step(time,6.1,0,6.101,-torq4j) \\ & +step(time,6,0,6.5,-2*torq2) \\ & +step(time,8.2,0,9,torq5j) \\ & +step(time,9.1,0,9.101,-torq5j) \\ & +step(time,9.2,0,9.5,torq) \\ & +step(time,11,0,12,-2*torq) \\ & +step(time,13.5,0,14,.catproject.torq6j) \\ & +step(time,14.1,0,14.101,-.catproject.torq6j) \\ & +step(time,14.2,0,14.5,torq). \end{aligned} \tag{14}$$

- Equation for the left front knee joint of the robot:

$$\begin{aligned} & step(\ time\ ,0.2\ ,0\ ,1.99\ ,torq2\ ) \\ & +step(time,2,0,2.01,torq2*-1) \\ & +step(time,2.1,0,2.2,torqt1) \end{aligned}$$

10.57647/ijm2c.2026.1603.15

$$+step(time,4{,}0{,}5,torq4j)$$
$$+step(time,5.1{,}0{,}5.101,torq4j*-1) \quad (15)$$
$$+step(time,6{,}0{,}7,torq5j)$$
$$+step(time,7.1{,}0{,}7.101,torq5j*-1)$$
$$+step(time,8{,}0{,}9,.catproject.torq6j)$$
$$+step(time,9.1{,}0{,}9.101,.catproject.torq6j*-1)$$
$$+step(time,9.3{,}0{,}9.4,torqt1*-1).$$

- Equation for the right back knee joint of the robot:

$$step(\ time\ ,0.2\ ,0\ ,1.99\ ,torq\ )$$
$$+step(time,2{,}0{,}2.01,torq*-1)$$
$$+step(time,2.1{,}0{,}2.2,torqt1*-1)$$
$$+step(time,4{,}0{,}5,torq4b)$$
$$+step(time,5.1{,}0{,}5.101,torq4b*-1) \quad (16)$$
$$+step(time,6{,}0{,}7,torq5b)$$
$$+step(time,7.1{,}0{,}7.101,torq5b*-1)$$
$$+step(time,8{,}0{,}9,.catproject.torq6b)$$
$$+step(time,9.1{,}0{,}9.101,.catproject.torq6b*-1)$$
$$+step(time,9.3{,}0{,}9.4,torqt1).$$

- Equation for the left back knee joint of the robot:

$$step(\ time\ ,0.2\ ,0\ ,1.99\ ,torq\ )$$
$$+step(time,2{,}0{,}2.01,torq*-1)$$
$$+step(time,2.1{,}0{,}2.2,torqt1*-1)$$
$$+step(time,4{,}0{,}5,torq4b)$$
$$+step(time,5.1{,}0{,}5.101,torq4b*-1) \quad (17)$$
$$+step(time,6{,}0{,}7,torq5b)$$
$$+step(time,7.1{,}0{,}7.101,torq5b*-1)$$
$$+step(time,8{,}0{,}9,.catproject.torq6b)$$
$$+step(time,9.1{,}0{,}9.101,.catproject.torq6b*-1)$$
$$+step(time,9.3{,}0{,}9.4,torqt1).$$

It should be noted that all conditions, including modeling, simulation, environmental conditions, etc., are exactly like a cat robot with a defective leg.

6. Result

After simulating and presenting the equations, the ADAMS software initiates the simulation process according to the equations and optimization parameters. Thanks to the presentation of accurate yet complex equations, the cat robot begins jumping up the stairs with a defective leg. Figure 8 and Figure 9 illustrates the various jumping steps of the cat robot with a healthy and defective leg on the stairs, respectively.

Looking at Figure 8, it can be seen that the cat robot with the healthy leg was able to successfully walk up the stairs and reach the upper terrace. Looking at the placement of the joint in the right back leg in Figure 9 and in Figure 10, the difference in the simulation performed in the two cases is clearly evident.

After simulating the ADAMS software, the software begins solving the problem and generates the best and most optimal state based on maximum and minimum values. After multiple executions, the software provides the values presented in Table 5.

Table 5 presents the optimum values of all defined parameters. All optimization studies reported in the manuscript (including the final defective-leg trajectory and the parametric study in Table 5) were executed at least three times with different initial guesses and random solver seeds. This procedure ensures that the results are not sensitive to the starting point or numerical noise.Convergence history of three independent optimization runs (different initial guesses and solver seeds) is shown in Figure 10.

A representative convergence history is shown in Figure 10, where three independent runs for minimizing the vertical distance between the right-front foot tip and the first stair platform consistently converge to the same optimal spring stiffness (k = 149.98 Nm/rad) and negligible final distance (<10 mm).

The optimized values obtained from the ADAMS software provide accurate simulation results of the robot's behavior during the jumping process. These values, derived from the dynamic equations that model the forces and torques acting on the robot's joints, take both internal and external effects into account.

By using these optimized values, the robot can achieve optimal performance under various conditions, particularly during jumping. These optimized values not only improve the robot's efficiency and stability but also reduce energy consumption and enhance the coordination of the robot's limbs. Moreover, with these optimized parameters, the robot can maintain optimal performance and stability in different situations and under varying forces.

The first step in analyzing the robot's movement is assessing the changes in the robot's center of mass. Figure 11 and Figure 12, illustrates the variations in the center of mass (Y direction and X direction) of the cat robot with a defective leg.

As depicted in Figure 11, the cat robot initiates the jump by adjusting its jump direction through the opening and closing of its joints.

This adjustment process continues until the robot reaches the upper terrace. Afterwards, the robot conserves and gradually releases power to execute jumps consecutively on each step. On the other hand, as seen in Figure 12, with the passage of time, the center of mass of the cat robot is closer to the origin of the coordinates and indicates the movement of the robot forward (against the X axis). To rigorously quantify the impact of the right-hind-leg defect and demonstrate the effectiveness of the fault-tolerant strategy, the optimized stair-jumping maneuver was executed in both the fully healthy (four functional legs) and defective configurations, respectively.

Figures 13 and 14 present a direct side-by-side comparison of the center-of-mass (CoM) trajectories in the sagittal plane for the healthy and defective-leg configurations, respectively.

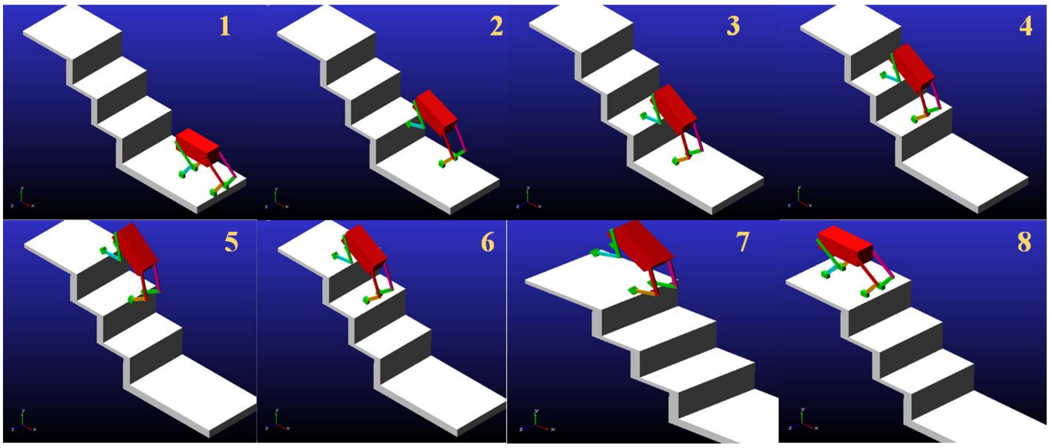

Figure 8. Cat robot jumping with a healthy leg on the stairs

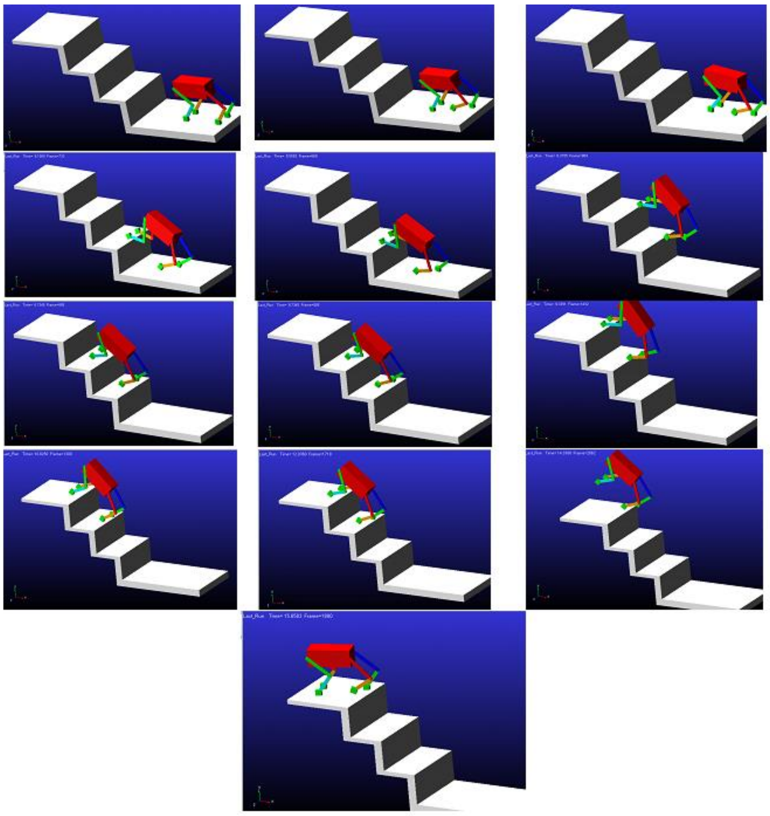

Figure 9. Cat robot jumping with a defective leg on the stairs

10.57647/ijm2c.2026.1603.15

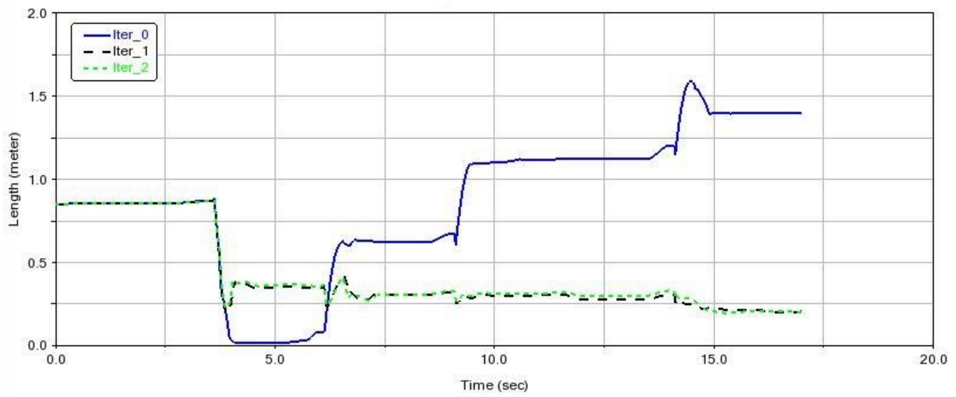

Figure 10. Convergence history of three independent optimization runs (different initial guesses and solver seeds)

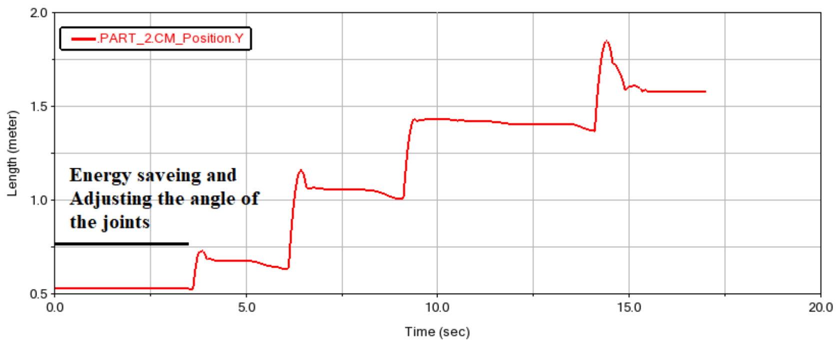

Figure 11. Variations of the CM-position of a cat robot with a defective leg (Y direction)

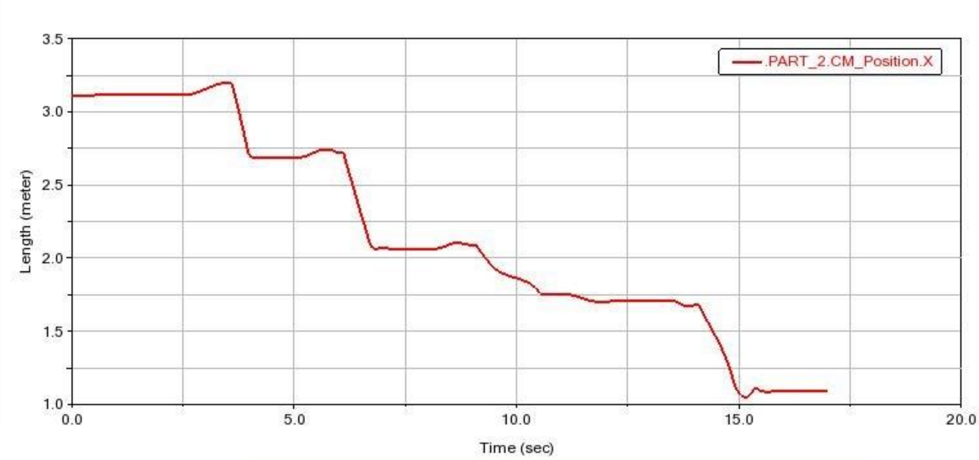

Figure 12. Variations of the CM-position of a cat robot with a defective leg (X direction)

The trajectories are visualized as 3D surfaces with time along the x-axis, vertical displacement (Z) along the y-axis, and forward displacement (X) encoded via the color gradient.

The vertical axis (Y-axis) represents the displacement of the robot's center of mass in the vertical direction (Z-direction). The colored lines illustrate how the center of mass simultaneously shifts in the horizontal direction (X-direction) over time. A comparison of the two figures shows that the defective leg introduces noticeable deviations in the three-dimensional CoM trajectory, increasing both vertical and horizontal oscillations during the jump.

In other word, despite the complete loss of active propulsion from one leg, the optimized strategy successfully completes the jump; however, the trajectory shows pronounced forward shift, significantly larger pitch excursion, and visible asymmetry as the remaining three legs compensate for both propulsion and stabilization. Another significant aspect in the analysis

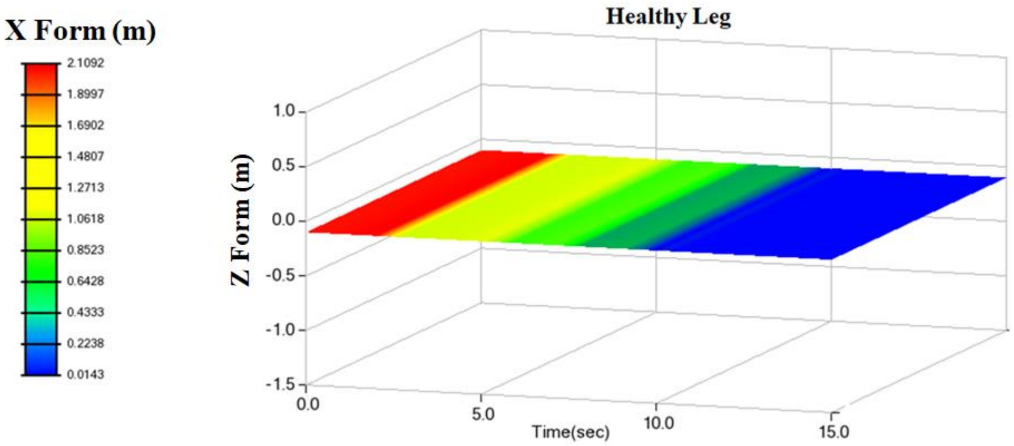

Figure 13. Center-of-mass (CoM) trajectories (Healthy leg)

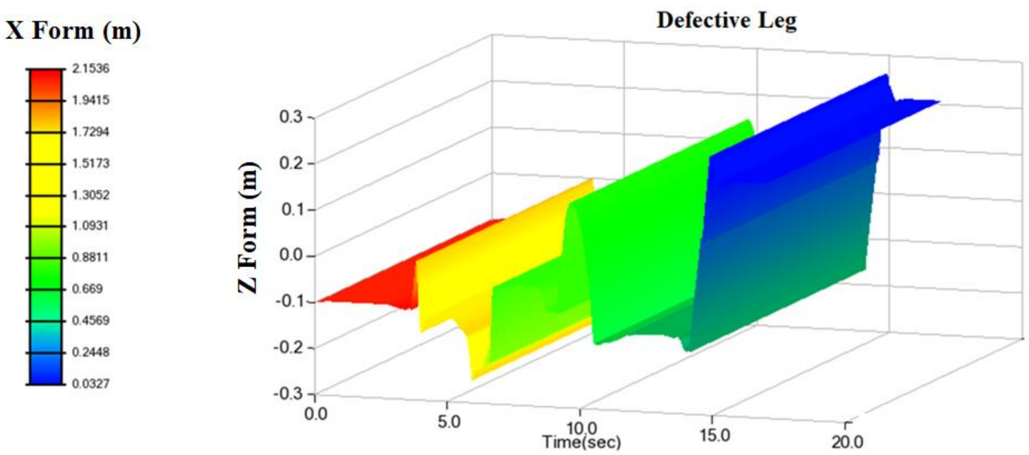

Figure 14. Center-of-mass (CoM) trajectories (Defective leg)

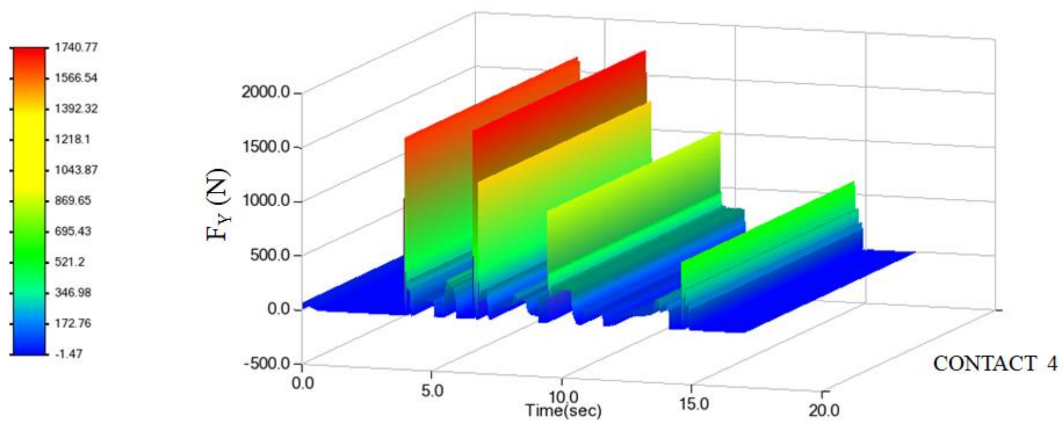

Figure 15. Contact force of the cat robot's defective leg

10.57647/ijm2c.2026.1603.15

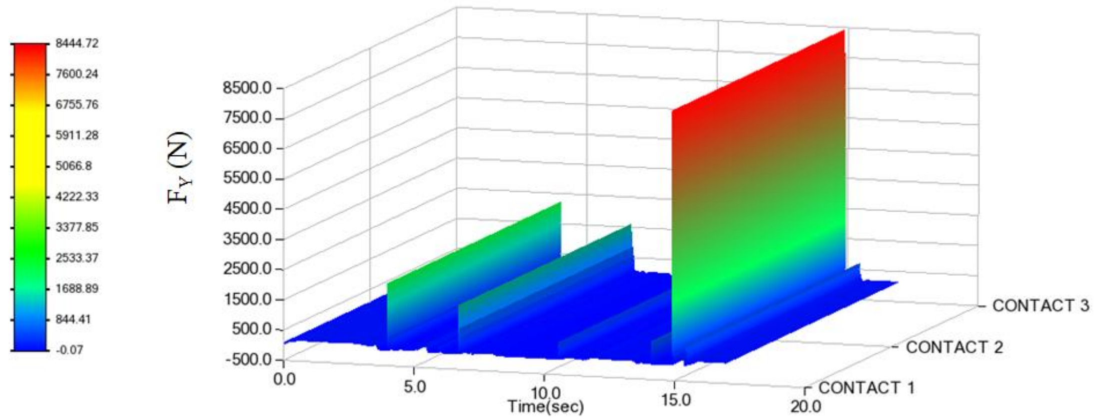

Figure 16. Contact force of the cat robot's legs

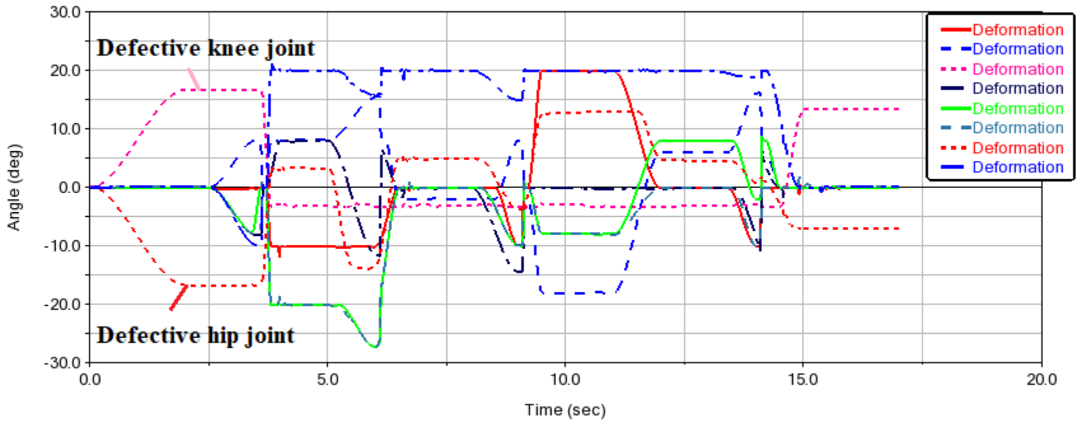

Figure 17. Deformation of the joint angle for a cat robot with a defective leg

Table 5. Optimized values

Design Variable	Optimized values
Stiffness	149.98
Damper	1
Torq	1199.31
Torq 2	1498.02
Torq e1	2500
Torq hb	649.800
Torq hb2	719.92
Torq h3	199.99
Torq 4F	1104.31
Torq 4b	2886.09
Torq 5f	1489.51
Torq 5b	2108.48
Torq 6f	1499.97
Torq 6b	2599.36

of the cat robot is the contact force exerted by its legs. Figures 15 and 16 present the contact force diagrams for the defective leg and the other legs of the robot, respectively.

According to Figures 15 and 16, it is evident that the defective leg of the cat robot initially remains raised off the ground due to its defect and does not make contact. However, as the robot jumps on the stairs, the defective leg has less contact with the surface compared to the other legs, indicating the lack of functionality in one of the back legs of the robot.

The degree of angle change in the joints of the cat robot is another crucial element in analyzing its jump. When one of the robot's legs is defective, the corresponding joint should exhibit a smaller change in angle compared to the rest of the joints. Figure 17 illustrates the angle change in the joints of the defective leg and the rest of the legs of the cat robot.

The provided figure illustrates the angular variations over time, clearly highlighting the differences caused by defects in the various joints. In this context, defects in the knee joint (represented by the red curve) and the hip joint (represented by the green curve) create notable disturbances in the robot's locomotion pattern, especially during the jumping and landing phases. The results show that, with defects in either of these joints, the robot struggles to maintain balance and perform jumps effectively, leading to abnormal joint angles and a reduction in performance when responding to sudden environmental changes.

This study not only offers a more precise analysis of cat robots with defective joints but also contributes to the development of novel approaches in designing robots capable of adapting to locomotion defects. Therefore, the findings of this study enhance our understanding of the effects of joint defects in robotic locomotion and provide solutions to improve the design of these robots in non-ideal and challenging conditions.

To objectively assess the performance of the proposed fault-tolerant stair-jumping strategy, Table 6 compares the achieved results with published data from leading high-performance and fault-tolerant quadruped platforms:

Table 6. Benchmarking against state-of-the-art robots

Robot / Study	Number of Leg	Mass (Kg)	Healthy → One-leg defective	Vertical jump - Stair / Obstacle height (m)	Dimensions of the robot body (m)
MIT Cheetah 3 [21]	4	45	Not tested	Desck (0.762)	0.60×0.25×0.20
Wang [1]	4	18.5	Not tested	No Jumping/ Obstacle- (0.145)	0.71×0.37×0.16
W-Leg [31]	2	21.2	Not tested	No Jumping/ Obstacle- (0.50)	0.50×0.44×0.20
Wujing Li [36]	4	28	Not tested	No Jumping/ Stair (0.175)	0.69×0.58×0.75
Li [29]	6	23	One Defective Leg	No Jumping/ Ramp- (0.175)	0.60×0.15×0.25
Mertyüz [28]	4	9.8	Not tested	No Jumping/Obstacle- (0.175)	0.43×0.24×0.26
NaghshNilchi [14]	4	45	Not tested	No Jumping/ Obstacle- (0.4)	0.6×0.25×0.2
Tatar [31]	2	21.2	Not tested	Obstacle (0.50)	0.50×0.44×0.20
Han [29]	4	12	Not tested	Obstacle (0.45)	0.50×.0.30×0.40
Proposed Model	4	36	Healthy Leg/One defective leg	0.60 (Stairs)	0.50×0.20×0.20

As shown in Table 6, while several state-of-the-art robots have demonstrated impressive dynamic capabilities in healthy conditions or limited fault scenarios (typically locked joints and obstacles ≤ 0.30 m), none have reported successful vertical stair jumping of 0.60 m height with a completely disabled hind leg. These results highlight the effectiveness of the presented optimization-based fault-tolerant strategy in addressing severe single-leg failure during highly dynamic maneuvers.

7. Conclusion

The ability to jump is highly important and practical for animals as it allows them to increase their speed and overcome obstacles. Taking inspiration from this natural movement behavior and simulating it in robotics can make significant contributions to the field. It is important to acknowledge that deformities in the legs of animals are not uncommon in nature. If a robot can be designed and simulated to continue its path despite having a defective leg and successfully reach its final destination through jumping, this robot could have widespread application.

This paper investigates the impact of a defective leg on the jumping performance of a quadruped robot on stairs. To achieve this, the dynamic equations of the system were derived using the Denavit-Hartenberg method, and the robot's kinematics were accurately modeled. Following this, a simulation of the robot's jump with a defective leg was conducted in the Adams software environment. The simulation effectively demonstrates the robot's behavior under realistic conditions with a defective leg.

The main innovation of this study lies in the combination of dynamic mathematical modeling with numerical simulation in ADAMS, which enables a more precise analysis of the robot's behavior under joint defects. In addition to the simulations, graphs were presented showing the changes in joint angles and robot position during the jump and landing phases. These graphs clearly illustrate the negative effects of a defective leg on the robot's balance and the ability to perform accurate jumps.

To summarize, the novelty of this paper lies in three major contributions:

- Successful consecutive stair jumping of a cat-sized quadruped robot (body mass 36 kg) using only three fully functional legs while one hind leg is completely non-functional (zero actuator torque and near-zero stiffness). All prior fault-tolerant jumping studies are limited to hexapod robots on low-incline slopes.
- Complete analytical derivation and implementation of eight separate joint-specific dynamic equations (Equations 13–20) for stair jumping with a defective hind leg. Previous quadruped jumping studies either assume all legs are healthy or do not provide joint-level equations under fault conditions.

This study is particularly innovative in the analysis of cat robots' performance under non-ideal conditions, such as joint defects. The simulation results show that defects in one leg significantly affect the robot's movement pattern, leading to reduced efficiency and stability. These findings can be directly applied to the design of quadruped robots that are resilient to joint defects and to improve control strategies for handling such conditions.

In conclusion, this study lays the foundation for new methods of simulating and analyzing the dynamics of cat robots with joint defects, and it has the potential to pave the way for the design of more resilient and adaptable robots in real-world, challenging environments.

Further areas of exploration and research in this field could include the jumping of the cat robot on different terrains, such as mineral stairs, as well as the walking motion and presence of a defective leg in the robot. These endeavors would undoubtedly yield valuable insights for the field of robotics.

Authors Contribution
All the authors have participated sufficiently in the intellectual content, conception and design of this work or the analysis and interpretation of the data (when applicable), as well as the writing of the manuscript.

Availability of data and materials
The data that support the findings of this study are available from the corresponding author, upon reasonable request.

Conflict of interests
The author states that there is no conflict of interest.

References

[1] Wang TH, Lin PC. A reduced-order-model-based motion selection strategy in a leg-wheel transformable robot. IEEE/ASME Trans Mechatron. 2022; 27(5): 3315–3321. doi: https://doi.org/10.1109/TMECH.2021.3126606

[2] Raibert MH. Legged robots that balance. MIT press; 1986.

[3] Berns K. The Walking Machine Catalogue. 2005.

[4] Todd DJ. Walking machines: an introduction to legged robots. Springer Science & Business Media; 2013.

[5] Ishino Y. Walking robot for underwater construction. In: Proc. Int. Conf. on Advanced Robotics; 1983. p. 107-114.

[6] Zykov V, Bongard J, Lipson H. Evolving dynamic gaits on a physical robot. In: Proceedings of Genetic and Evolutionary Computation Conference, Late Breaking Paper, GECCO; vol. 4. 2004. p. 2004.

[7] Bruzzone L, Quaglia G. Locomotion systems for ground mobile robots in unstructured environments. Mech Sci. 2012; 3(2): 49–62. doi: https://doi.org/10.5194/ms-3-49-2012

[8] Rongfu L, Guo W, Li M. Novel design of legged mobile landers with decoupled landing and walking functions containing a rhombus joint. J Mech Robot. 2018; 10(6): 061017. doi: https://doi.org/10.1115/1.4040413

[9] Dominik B, Labecki P, Skrzypczyński P. An exploration-based approach to terrain traversability assessment for a walking robot. In: 2013 IEEE International Symposium on Safety, Security, and Rescue Robotics (SSRR); 2013. p. 1-6. IEEE.

[10] Takahide Y, Kuroda M, Ujino R, Kaneko H, Higuchi H, Iwasaki S, Kanemoto Y, Asatani M, Koshiishi T. Development of experimental legged robot for inspection and disaster response in plants. In: 2017 IEEE/RSJ International Conference on Intelligent Robots and Systems (IROS); 2017. p. 4869-4876. IEEE.

[11] Luca B, Quaglia G. Locomotion systems for ground mobile robots in unstructured environments. Mech Sci. 2012; 3(2): 49–62. doi: https://doi.org/10.5194/ms-3-49-2012

[12] Robertas D, Maskeliūnas R, Narvydas G, Narbutaitė R, Połap D, Woźniak M. Intelligent automation of dental material analysis using robotic arm with jerk optimized trajectory. J Ambient Intell Humanized Comput. 2020; 11: 6223-6234. doi: https://doi.org/10.1007/s12652-020-02605-8

[13] WeiHai Ch, Ren G, Wang J, Liu D. An adaptive locomotion controller for a hexapod robot: CPG, kinematics and force feedback. Sci China Inf Sci. 2014; 57: 1–18. doi: https://doi.org/10.1007/s11432-014-5148-y

[14] Weitao X, Yesilevskiy Y, Remy CD. Selecting gaits for economical locomotion of legged robots. Int J Robot Res. 2016; 35(9): 1140–1154. doi: https://doi.org/10.1177/0278364915612572

[15] NaghshNilchi M, Saadat M, Soleimani A, Vahabi M, Salehi M. Modeling and simulation of a jumping four-legged robot on staircases. J Appl Dyn Syst Control. 2024; 4(4): 9.

[16] Quan N, Powell M, Katz B, Di Carlo J, Kim S. Optimized jumping on the MIT Cheetah 3 robot. In: 2019 Int Conf on Robotics and Automation (ICRA); 2019. p. 7448-7454. IEEE. doi: https://doi.org/10.1109/ICRA.2019.8794449

[17] Xu B, Zhang X, Yu X, Ou Y, Zhang K, Cai H, Zhao J, Fan J. A motion planner based on Mask-D3QN of quadruped robot motion for steam generator. Biomimetics. 2024 ;9(10): 592.

[18] Ribeiro JC, Dias B, Lopes G, Flores P. Trends in the control of hexapod robots: a survey. Robotics. 2021; 10(3): 100. doi: https://doi.org/ 10.3390/robotics10030100

[19] Ayonga H, Harib O, Hartley R, Gong Y, Grizzle J. Rapid trajectory optimization using C-FROST with illustration on a Cassie-series dynamic walking biped. In: 2019 IEEE/RSJ Int Conf on Intelligent Robots and Systems (IROS); 2019. p. 4722-4729. IEEE. doi: https://doi.org/10.1109/IROS40897.2019.8968056

[20] Joel Ch, Lau M, Cheung G, Kuffner J, Hodgins J, Kanade T. Footstep planning for the Honda ASIMO humanoid. In: Proc IEEE Int Conf on Robotics and Automation; 2005. p. 629-634. IEEE. doi: https://doi.org/10.1109/ROBOT.2005.1570188

[21] Powell B, Katz B, Di Carlo J, Wensing P, Kim S, Matthew J. MIT Cheetah 3: Design and control of a robust, dynamic quadruped robot. In: 2018 IEEE/RSJ Int Conf on Intelligent Robots and Systems (IROS); 2018: 2245-2252. doi: https://doi.org/10.1109/IROS.2018.8593885

[22] Tianjiao L, Ye Sh, Chen L, Sun C, Zhang A. Energy efficient swing leg trajectory planning for quadruped robots walking on rough terrain. In: 2019 IEEE Int Conf on Robotics and Biomimetics (ROBIO); 2019. p. 2128-2133. IEEE.

[23] McGuire K, Wagter Ch, Tuyls K, Kappen H, de Croon GC. Minimal navigation solution for a swarm of tiny flying robots to explore an unknown environment. Sci Robot. 2019; 4(35): 9710. doi: https://doi.org/10.1126/scirobotics.aax9710

[24] Guoteng Zh, Rong X, Hui Ch, Li Y, Li B. Torso motion control and toe trajectory generation of a trotting quadruped robot based on virtual model control. Adv Robot. 2016; 30(4): 284–297.

[25] Linqi Y, Liu H, Wang X, Liang B, Yuan B. Multi-task control for a quadruped robot with changeable leg configuration. In: 2020 IEEE/RSJ Int Conf on Intelligent Robots and Systems (IROS); 2020. p. 3944-3950. IEEE.

[26] Min Sung A, Chae H, Hong DW. Stable, autonomous, unknown terrain locomotion for quadrupeds based on visual feedback and mixed-integer convex optimization. In: 2018 IEEE/RSJ Int Conf on Intelligent Robots and Systems (IROS); 2018. p. 3791-3798. IEEE.

[27] Liheng M, Gao F, Tian Y, Zhao Y. Novel method for preventing shin-collisions in six-legged robots by utilizing a robot–terrain interference model. Mech Mach Theory. 2020; 151: 103897. doi: https://doi.org/10.1016/j.mechmachtheory.2020.103897

[28] Mertyüz İ, Tanyıldızı AK, Taşar B, Tatar AB, Yakut O. FUHAR: A transformable wheel-legged hybrid mobile robot. Robot Auton Syst. 2020; 133: 103471. doi: https://doi.org/10.1016/j.robot.2020.103471

[29] Tao L, Fan X, Liu Y, Jia X, Deng Y. Hexapod robot fault tolerant gait on slope and simulation verification. In: J Phys Conf Ser. vol. 1601. IOP Publishing; 2020. p. 062038. doi: https://doi.org/10.1088/1742-6596/1601/6/062038

[30] Debabrata S, Kumar Dubey Sh, Mahapatra A, Shekhar Roy Sh. Modeling and analysis of fault tolerant gait of a multi-legged robot moving on an inclined plane. Procedia Technol. 2014; 14: 93–99.

[31] Tatar AB. W-leg jumping robot: Mechanical design, dynamical analysis and simulation of jumping dual wheel-leg hybrid robot. Arab J Sci Eng. 2024; 49(11): 15463–15481. doi: https://doi.org/10.1007/s13369-024-08882-5

[32] Han J, Wan B, Zheng Y, Song Z. An energy-efficient obstacle-crossing control framework for quadruped robots. Results Eng. 2025.

[33] Li H, Qi C, Mao L, Zhao Y, Chen X, Gao F. Staircase-climbing capability-based dimension design of a hexapod robot. Mech Mach Theory. 2021; 164: 106200. doi: https://doi.org/10.1016/j.mechmachtheory.2021.104400

[34] Li W, Wei L, Zhang X. A wheels-on-knees quadruped assistive robot to carry loads. Appl Sci. 2022; 12(18): 9386. doi: https://doi.org/10.3390/app12189386

[35] Roy F. Rigid body dynamics algorithms. Springer; 2014.

[36] Sciavicco L, Siciliano B, Sciavicco B. Modelling and Control of Robot Manipulators. Springer-Verlag, Heidelberg; 2000.